

Core-Level X-Ray Photoemission Satellites in Ruthenates: A New Mechanism Revealing the Mott Transition

Hyeong-Do Kim,¹ Han-Jin Noh,² K.-H. Kim,² and S.-J. Oh^{2,*}

¹*Pohang Accelerator Laboratory, Pohang University of Science and Technology, Pohang 790-784, Korea*

²*School of Physics and Center for Strongly Correlated Materials Research,
Seoul National University, Seoul 151-742, Korea*

(Dated: October 29, 2018)

Ru 3d core-level x-ray photoemission spectra of various ruthenates are examined. They show in general two-peak structures, which can be assigned as the screened and unscreened peaks. The screened peak is absent in a Mott insulator, but develops into a main peak in the metallic regime. This spectral behavior is well explained by the dynamical mean-field theory calculation for the single-band Hubbard model with on-site core-hole potential using the exact diagonalization method. The new mechanism of the core-level photoemission satellite can be utilized to reveal the Mott transition phenomenon in various strongly correlated electron systems, especially in nano-scale devices and phase-separated materials.

PACS numbers: 71.10.Fd, 71.30.+h, 79.60.-i

Core-level x-ray photoemission spectroscopy (XPS) has long been a powerful tool to investigate the chemical environment of solids and molecules [1]. Usually the variation of the binding energy depending on the chemical environment (“chemical shift”) is utilized for this purpose, but satellite structures arising from the Coulomb attraction between valence electrons and a core hole created in photoemission can be a fruitful source of information, especially in strongly correlated systems such as rare-earth [2] and transition-metal compounds (TMCs) [3, 4]. A good example is the high- T_c and related cuprates [4], where the satellite structures of Cu 2p core-level XPS have been instrumental to confirm the charge-transfer nature of the insulating gap in the parent compounds which were traditionally classified as Mott insulators [5], and determine basic parameters such as the d - d Coulomb correlation energy and the charge-transfer energy.

Such a strong electron correlation effect has been considered to be weak in 4d TMCs because 4d orbitals are fairly delocalized, and RuO₂, for example, is traditionally classified as a band metal [6]. However, recent studies revealed that many ruthenates such as Ca_{2-x}Sr_xRuO₄ [7] and pyrochlores [8, 9] have various interesting properties related with the correlation effect among Ru 4d electrons. Ru 3d core-level XPS spectra also show some hint of the strongly correlated nature of Ru 4d electrons. As shown in Fig. 1, the Ru 3d spin-orbit doublet, of which splitting is about 4 eV, consists of roughly two components, “screened” (denoted as “s”) and “unscreened” (denoted as “u”) peaks in various ruthenates [10, 11, 12] including RuO₂ where their origin has been the subject of a long debate [10, 11, 12, 13, 14]. The peak “s”, located at about 2 eV lower binding energy than that of the rather broad unscreened peak “u”, is absent in an insulator Y₂Ru₂O₇ and grows as the system becomes more metallic. Hence Cox *et al.* suggested that the peak “s” might originate from the screening of a core hole by a

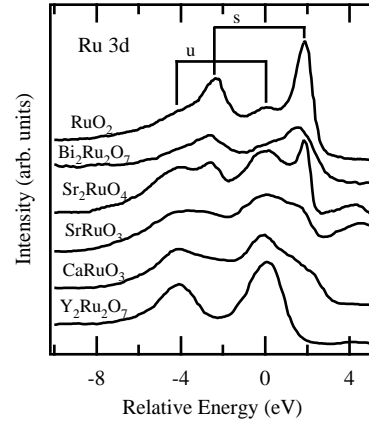


FIG. 1: Ru 3d XPS spectra of RuO₂ (after [10]), Bi₂Ru₂O₇ (after [11]), Sr₂RuO₄ (after [12]), SrRuO₃, CaRuO₃, Y₂Ru₂O₇ (after [11]). “s” and “u” denote screened and unscreened peaks, respectively, following [11]. All the spectra are aligned by the unscreened-peak positions of Ru 3d_{5/2}.

quasiparticle at E_F [11]. On the other hand, we may attribute it to the charge-transfer mechanism as in 3d TMCs, but the energy separation between the main and satellite peaks is much smaller than that of a Pd 3d spectrum in PdO [15], while we expect larger separation according to the chemical trend [3]. Quite recently, Okada [14] tried to explain the two-peak structure in Sr₂RuO₄ [12] by the “non-local screening” effect [16] in addition to the charge-transfer mechanism. He could not, however, fit the strong intensity variation and the little change of the energy separation in ruthenate series with reasonable values of parameters.

In this Letter, we propose a new mechanism for the two-peak structures in the Ru 3d core-level XPS spectra of ruthenates based on a single-band Hubbard model. The core-level spectra of a single-band Hubbard model with core-hole potential are calculated by the dynamical

cal mean-field theory (DMFT) [17]. The DMFT can describe successfully the Mott transition with the change of ratio of the Coulomb interaction U between conduction electrons to the band width W , and it should be suitable for a local problem like core-level XPS despite its shortcomings due to “local” electron self-energy [18]. In this picture, the “screened” peak originates from the screening of a core-hole by quasiparticles on the Fermi surface. We found that the calculation can reproduce the spectral behavior shown in Fig. 1 just by changing the correlation strength with reasonable parameter values. We also made a systematic study of the Ru $3d$ XPS spectra of a bandwidth-controlled Mott-Hubbard system $Y_{2-x}Bi_xRu_2O_7$ [9] as a function of composition to strengthen our conclusion.

We start from the single-band Hubbard model

$$H = \sum_{k\sigma} \epsilon_k a_{k\sigma}^\dagger a_{k\sigma} + U \sum_i n_{i\uparrow} n_{i\downarrow}, \quad (1)$$

where the notation is standard, which is exactly mapped in infinite dimensions on to the single-impurity Anderson model according to the DMFT [17]

$$H_{\text{And}} = \sum_{l=2,\sigma}^{N_s} \tilde{\epsilon}_l c_{l\sigma}^\dagger c_{l\sigma} + \epsilon_d \sum_{\sigma} d_{\sigma}^\dagger d_{\sigma} + U n_{d\uparrow} n_{d\downarrow} + \sum_{l\sigma} V_l (c_{l\sigma}^\dagger d_{\sigma} + \text{H.c.}). \quad (2)$$

In order to describe a core-level spectrum, we should add a term due to a core hole for XPS final states after getting the converged model parameters,

$$H_{\text{core}} = (\epsilon_h - Q \sum_{\sigma} d_{\sigma}^\dagger d_{\sigma}) h^\dagger h, \quad (3)$$

where the operator h^\dagger (h) creates (destroys) a core hole on the “impurity” site, ϵ_h is a core-hole energy, and Q ($\equiv 1.25U$, for simplicity in all calculations) is the Coulomb interaction between the core-hole and “impurity-site” conduction electrons. In order to solve the model with the semi-elliptical shape for the conduction-band density of states, we followed the exact diagonalization method proposed by Caffarel and Krauth [19].

Figure 2 shows core-level and valence-band spectra of the ten-site ($N_s = 10$) half-filled model obtained by the modified Lanczos method changing the ratio W/U from a Mott insulator regime to a good metal regime to show the behavior of spectral weights in the bandwidth-controlled metal-insulator transition. For this particle-hole symmetric model, ϵ_d is chosen to be $-U/2$, then the chemical potential μ is identically zero. The core-hole energy ϵ_h is set to Q . The core-level spectra are mainly composed of two peaks (minor peaks are due to the finite size) and their behavior with W/U is quite similar to that of the valence-band spectra and, moreover, the intensity of the “screened peak” is found to be nearly

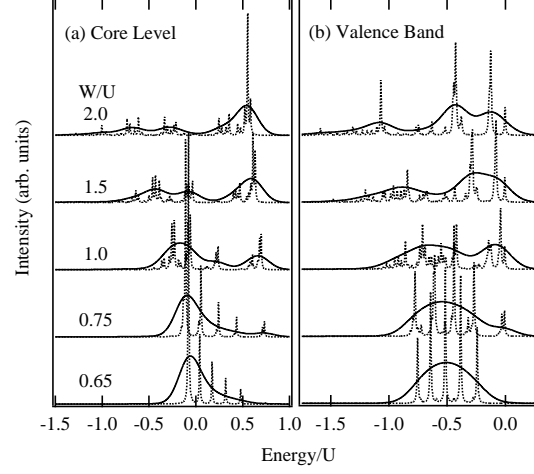


FIG. 2: (a) Core-level and (b) valence-band spectra of the half-filled Hubbard model with $N_s = 10$ calculated by the DMFT varying W/U . Solid lines are guidelines obtained by broadening dotted lines with a Gaussian of 0.25 full width at half maximum to remove discreteness due to the finite size.

proportional to the quasiparticle weight Z calculated by $(1 - \frac{\partial \text{Im}\Sigma(i\omega)}{\partial \omega})^{-1}|_{\omega \rightarrow 0}$, which implies that the two-peak structure is strongly related with the Mott transition. In a Mott insulator ($W/U = 0.65$) we can see a broad single peak, and as the coherent peak grows with the increase of W in the valence-band spectra, a sharp shake-down satellite structure appears in the core-level spectra in the positive energy side and eventually becomes a main peak with the asymmetric low-energy tail. Around $W/U = 2.0$ (top-most figure), both the core-level and valence-band spectra remind of the famous 6 eV satellite in Ni metal, which is explained by the Mahan-Nozières-DeDominicis model with strong core-hole potential for the former and by the Hubbard model for the latter [20]. Now, both spectra are explained in a single model thanks to the DMFT based on the exact diagonalization, and it should be applicable to other strongly correlated systems showing the Mott transition.

In order to investigate in detail the origin of the two-peak structure in the core-level spectra, we obtained all the eigenvalues and eigenvectors of the initial and final states of a four-site model by explicit exact diagonalization. Figure 3 shows the calculated core-level spectra for the case of (a) $W/U = 0.75$ and (b) 1.5. Here we see again that for a narrow band case (a) only the unscreened peak is dominant, while for the wide band (b) both screened and unscreened peaks appear in the core-level spectra. To understand the valence-electron configuration of these different core-level final states, we plot at the bottom of the figure the bar diagram showing the weights of various valence-electron configurations contributing to each core-level peak. For the four-site model, we should consider three energy levels in the conduction band representing a lower Hubbard band (LHB), a coherent peak, and an

upper Hubbard band, along with the “impurity” level at the core-hole site in the presence of a core-hole. Then there are three major valence-electron configurations in the XPS final state, i.e. d^1 ($\equiv d^1L^2C^1$, for $N_s = 4$), $d^2\bar{C}$, and $d^2\bar{L}$, where d denotes the “impurity” level and C (L) denote the coherent peak (LHB). These valence-electron configurations are shown schematically in Fig. 4. It can be easily noticed from the bar diagram at the bottom of Fig. 3 that the unscreened peak originates from the configuration d^1 , while the screened peak from the configurations $d^2\bar{C}$ and $d^2\bar{L}$.

With these configurations, the behavior of two-peak structure with the change of W/U is simply understood. When W/U is so small that the system becomes a Mott insulator, the configuration $d^2\bar{C}$ is absent both in the ground and the final states, so the unscreened peak, of which main configuration is d^1 , becomes dominant, and the screened peak by the configuration $d^2\bar{L}$ is located near the unscreened peak (the separation is $Q - U$ in the limit $W/U \rightarrow 0$). Since the configuration $d^2\bar{L}$ represents a single-hole state in the LHB, the core-level peak of a Mott insulator has extra linewidth broadening reflecting the LHB shape. When W/U is close to the critical value and the system becomes a metal, the configuration $d^2\bar{C}$ is now available to take part in the screening of the core hole, which makes a sharp shake-down satellite peak, whose energy is about $Q - U/2$ lower than that of the unscreened peak and its intensity increases with the weight of the coherent peak.

To test the validity of the present model, we made a systematic study of the Ru $3d$ core-levels in $Y_{2-x}Bi_xRu_2O_7$ system. This system is known to be a bandwidth-controlled Mott-Hubbard system from theoretical calculation [9], transport properties [8] and valence-band photoelectron spectra [21], which shows the metal-insulator transition around $x = 0.9$ [8]. We took Ru $3d$ XPS spectra of polycrystalline $Y_{2-x}Bi_xRu_2O_7$

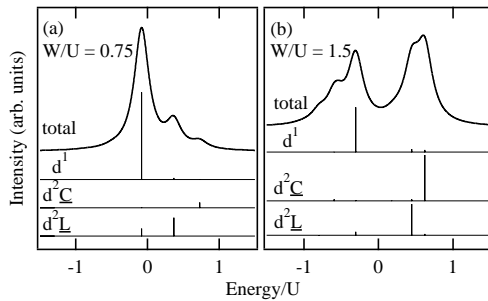


FIG. 3: Core-level spectra in the four-site model for (a) $W/U = 0.75$ and (b) 1.5 . The calculated spectra are broadened by a Lorentzian of 0.25 full width at half maximum. The bar diagram at the bottom indicates the weights of different valence-electron configurations in each XPS final state. The three valence-electron configurations d^1 , $d^2\bar{C}$, and $d^2\bar{L}$ are shown schematically in Fig. 3.

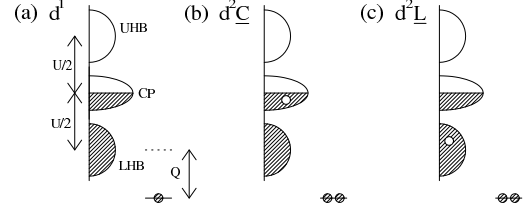


FIG. 4: Schematic diagrams of three major valence-electron configurations contributing to the core-level spectra. Note that the “impurity” level at the core-hole site is lowered by the attractive Coulomb potential Q .

samples ($x = 0.0, 0.4, 1.0, 1.6$, and 2.0) using Mg $K\alpha$ source after annealing four hours under the oxygen partial pressure of 10^{-5} Torr at 900 K. The annealing process, which removes almost all of the carbon contaminations in the sample, is essential because the binding energy of the Ru $3d$ core-level is close to that of C $1s$ peak.

Ru $3d$ XPS spectra (solid lines) of $Y_{2-x}Bi_xRu_2O_7$ thus obtained are shown in Fig. 5 (a) after removing the inelastic background and the small residual C $1s$ peak contribution by deconvolution using Doniach-Šunšić line shapes. We can see the systematic behavior that the weight of the screened peak becomes larger as the Bi concentration increases. This tendency is strongly correlated with the transport properties [8] and valence-band photoelectron spectra [21]. Using the present model, the core-level spectra of $Y_{2-x}Bi_xRu_2O_7$ series could be reproduced by changing only W with fixed U value ($= 1.7$ eV). We also fit the spectra of other ruthenates shown in Fig. 1 by freeing U , and Table 1 summarizes all the parameter values. After proper broadening of calculation results by a Voigt function to simulate the core-hole lifetime and the experimental resolution, final results (dotted lines) are plotted over the experimental spectra in Fig. 5 (a)

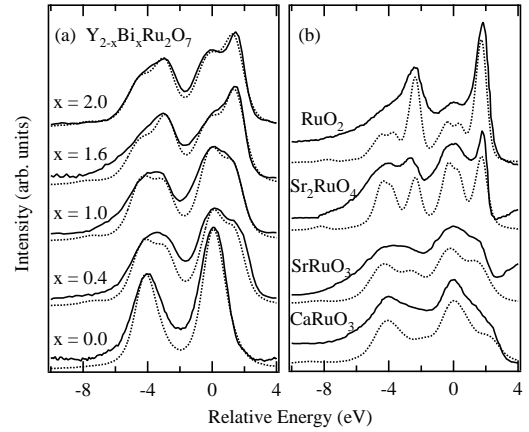


FIG. 5: Comparison of Ru $3d$ XPS spectra (solid lines) of (a) $Y_{2-x}Bi_xRu_2O_7$ and (b) other ruthenates with the present model calculations (dotted lines). See text for details.

$Y_{2-x}Bi_xRu_2O_7$ and (b) other ruthenates. The fitting results are quite satisfactory and all the spectral behaviors are well reproduced. Rather surprisingly, RuO_2 , which was believed to be well described by band calculations [6], should be reconsidered as a strongly correlated metal according to our fitting result ($W/U = 2.0$).

Although the present model does not include such terms as $4d$ -orbital degeneracy and also the $Ru\ 4d_{t_{2g}}$ band shape is far from semi-elliptical [22, 23], it is quite successful in describing the two-peak structure of the core-level spectra, which confirms that the Mott-Hubbard mechanism is the most important factor. Nevertheless, the role of $O\ 2p$ bands could not be ruled out in two respects: (1) The change of W -value for $Y_{2-x}Bi_xRu_2O_7$ is rather larger than expected [9, 22], while W values for other ruthenates are comparable to those of band calculations [23]. Since we are dealing with an *effective* Hubbard model, in which $O\ 2p$ bands are integrated out, the U value should change in real materials depending on the $Ru\ 4d$ - $O\ 2p$ hybridization strength, which would result in the reduction of the W variation. (2) We may expect that a similar two-peak structure should appear in other strongly correlated TMCs. Actually, there is some hint of it in Ti_2O_3 [24] and V_2O_3 [25]. But the screened-peak intensity is rather small in these systems compared with the coherent peak of the valence band [26], which may be explained by the competition between the charge-transfer screening by the $O\ 2p$ electron and the screening by quasiparticles at E_F . Since the quasiparticle screening takes place through mediating $O\ 2p$ orbitals, it is probably more rapidly suppressed than the charge-transfer screening as the hybridization strength becomes weak. Further experimental and theoretical studies are necessary to clarify this issue.

In summary, we have elucidated the origin of two-peak structures in the $Ru\ 3d$ core-level XPS spectra of various ruthenates as due to the different screening mechanisms in the Mott-Hubbard picture of the metal-insulator transition. This mechanism should be applicable to other TMCs as well, hence core-level XPS can be utilized to distinguish metallic from insulating regions in phase-separated materials [27] and TMC-based nano-electronic devices when used in conjunction with spectro-microscopic tools such as scanning photoemission microscopy.

This work was supported in part by the Korea Sci-

ence and Engineering Foundation through the Center for Strongly Correlated Materials Research of Seoul National University and by the Korea Ministry of Science and Technology.

[*] Corresponding author.

- [1] T. A. Carlson, *Photoelectron and Auger Spectroscopy* (Plenum Press, New York, 1975); M. Cardona and L. Ley in *Photoemission in Solids I* (Springer-Verlag, Berlin, 1978).
- [2] O. Gunnarsson and K. Schönhammer, Phys. Rev. Lett. **50**, 604 (1983); J. W. Allen *et al.*, Adv. Phys. **35**, 275 (1986).
- [3] J. Zaanen, C. Westra, and G. A. Sawatzky, Phys. Rev. B **33**, 8060 (1986); J. Park *et al.*, Phys. Rev. B **37**, 10867 (1988); G. Lee and S.-J. Oh, Phys. Rev. B **43**, 14674 (1991); A. E. Bocquet *et al.*, Phys. Rev. B **46**, 3771 (1992).
- [4] Z.-X. Shen *et al.*, Phys. Rev. B **36**, 8414 (1987).
- [5] N. F. Mott, *Metal-Insulator Transitions* (Taylor and Francis, New York, 1990).
- [6] R. R. Daniels *et al.*, Phys. Rev. B **29**, 1813 (1984).
- [7] S. Nakatsuji and Y. Maeno, Phys. Rev. Lett. **84**, 2666 (2000).
- [8] R. Kanno *et al.*, J. Solid State Chem. **102**, 106 (1993); S. Yoshii and M. Sato, J. Phys. Soc. Jpn. **68**, 3034 (1999).
- [9] K.-S. Lee, D.-K. Seo, and M.-H. Whangbo, J. Solid State Chem. **131**, 405 (1997).
- [10] Y. J. Kim, Y. Gao, and S. A. Chambers, Appl. Surf. Sci. **120**, 250 (1997).
- [11] P. A. Cox *et al.*, J. Phys. C: Solid State Phys. **16**, 6221 (1983).
- [12] A. Sekiyama, *Abstracts of the Meeting of the Phys. Soc. Jpn* (55th Annual Meeting, Niigata, Sep. 2000); recited from [14].
- [13] K. S. Kim and N. Winograd, J. Catal. **35**, 66 (1974); H. J. Lewerenz, S. Stucki, and R. Kotz, Surf. Sci. **126**, 893 (1983); K. Reuter and M. Scheffler, Surf. Sci. **490**, 20 (2001); H. Over *et al.*, Surf. Sci. **504**, L196 (2002).
- [14] K. Okada, Surf. Rev. Lett. **9**, 1023 (2002).
- [15] T. Uozumi *et al.*, J. Phys. Soc. Jpn. **69**, 1226 (2000).
- [16] M. A. van Veenendaal and G. A. Sawatzky, Phys. Rev. Lett. **70**, 2459 (1993).
- [17] For a review, see A. Georges *et al.*, Rev. Mod. Phys. **68**, 13 (1996).
- [18] I. H. Inoue *et al.*, Phys. Rev. Lett. **74**, 2539 (1995).
- [19] M. Caffarel and W. Krauth, Phys. Rev. Lett. **72**, 1545 (1994).
- [20] For a review, see L. C. Davis, J. Appl. Phys. **59**, R25 (1986).
- [21] J. Park, Ph.D thesis, Seoul National University, 2001.
- [22] F. Ishii and T. Oguchi, J. Phys. Soc. Jpn. **69**, 526 (2000).
- [23] K. M. Glassford and J. R. Chelikowsky, Phys. Rev. B **47**, 1732 (1993); T. Oguchi, Phys. Rev. B **51**, 1385 (1995); I. I. Mazin and D. J. Singh, Phys. Rev. B **56**, 2556 (1997).
- [24] T. Uozumi *et al.*, J. Phys. Soc. Jpn. **65**, 1150 (1996).
- [25] J.-H. Park, Ph.D. thesis, University of Michigan, 1994.
- [26] S.-K. Mo *et al.*, Phys. Rev. Lett. **90**, 186403 (2003).
- [27] N. Mathur and P. Littlewood, Phys. Today **56**, 25 (2003).

TABLE I: Parameter values (in eV) obtained from fitting $Ru\ 3d$ XPS spectra of ruthenates.

x in $Y_{2-x}Bi_xRu_2O_7$	U	W		U	W
0.0	1.7	1.2	$CaRuO_3$	2.7	2.6
0.4	1.7	2.1	$SrRuO_3$	2.15	2.6
1.0	1.7	2.15	Sr_2RuO_4	2.15	2.8
1.6	1.7	2.9	RuO_2	1.8	3.6
2.0	1.7	2.7			